DOE/NASA/3186-1
NASA CR-165186

Performance Prediction of Straight Two-Dimensional Diffusers

Mahesh S. Greywall
Wichita State University
Wichita, Kansas 67208

September 1980

Prepared for
National Aeronautics and Space Administration
Lewis Research Center
Cleveland, Ohio 44135
Under Grant NSG-3186

for
U.S. DEPARTMENT OF ENERGY
Fossil Energy
Office of Magnetohydrodynamics
Washington, D.C. 20545
Under Interagency Agreement DE-AI01-77ET10769

INTRODUCTION

A diffuser is a passive fluid device whose primary function is to convert the kinetic energy of a fluid into static pressure. It is a key element in centrifugal compressors and in power systems using expansion devices. In centrifugal compressors energy is imparted to the fluid initially as kinetic energy. The accelerated fluid is then slowed down through diffusing passages to increase its static pressure. In power systems using expansion devices such as turbines and magnetohydrodynamic generator channels the available exit pressure is fixed by the background. By attaching a diffuser to the end of the expansion device, part of the kinetic energy of the working fluid leaving the device can be converted into static pressure thus reducing the pressure at the exit of the expansion device below the available background pressure. Since the efficiency of such power systems is a function of the pressure ratio across the expansion device, a decrease in the exit pressure of the device significantly increases the efficiency for a given inlet pressure.

Considerable amount of experimental work has been carried out to determine the performance of straight two-dimensional diffusers [1,2,3,4]. Based on the results of these investigations Runstadler-Dean [4], and Reneau-Johnston-Kline [5] have generated diffuser performance maps to aid the designer. Attempts to theoretically predict diffuser performance have so far met with limited success. In order to better understand the diffuser flow and to predict diffuser performance when the design conditions (in particular diffusers with very large inlet blockage and heat transfer to

the walls as encountered in magnetohydrodynamic power generation applications) are outside the range of available experimental data there is need to develop theoretical methods to predict diffuser performance. Reliable theoretical methods to predict diffuser performance will also aid in exploring various ideas put forward to increase diffuser efficiencies.

In the present work we have calculated pressure recovery coefficients along with other flow parameters for the diffuser geometries and the inlet flow conditions experimentally investigated in Refs. [1,2,3,4]. By comparing the calculated and experimental results we have derived an algorithm to theoretically predict diffuser performance. The calculations were carried out using the method of Greywall [6]. This method performs full viscous calculations, that is it calculates flow in a channel without separating it into a boundary layer and a core. Key points of the computational methodology of special significance to the diffuser calculations presented in this study are given in Appendix B.

COMPARISON OF IDEAL, CALCULATED, AND MEASURED C_p

We follow the standard definition of pressure recovery coefficient, C_p,

$$C_p = \frac{p_e - p_i}{p_{0i} - p_i} \quad ,$$

where p_e and p_i are the diffuser exit and inlet static pressures, and p_{0i} is the inlet stagnation pressure.

Consider an incompressible and inviscid flow through a diffuser. We assume that at the diffuser entrance the velocity distribution normal to the flow is uniform (no boundary layer). Then, since the flow is inviscid, the velocity distribution will remain uniform as the flow proceeds along the diffuser. For such a flow application of continuity and Bernoulli's equaltion yields the ideal pressure recovery coefficient, C_{pi},

$$C_{pi} = 1 - \frac{1}{AR^2} \quad ,$$

where AR is the ratio of the exit to the inlet diffuser areas. Later on AR will be referred to as the geometric area ratio.

In Fig. 1 we have graphed C_{pi} as a function of AR. Also shown in this figure are C_{pt}, the pressure recovery coefficient we calculated, and C_{pm}, the measured pressure recovery coefficient from Ref. [2]. Geometry of the diffuser and the inlet flow conditions used in the calculation of C_{pt} were identical to those used for the experimental C_{pm}. The flow conditions for C_{pt} and C_{pm} are such that the flow can be considered incompressible. The diffuser length, L,

is equal to 12 times $2H_0$, where H_0 is half the distance at the inlet between the diverging diffuser walls. The boundary layer displacement thickness at the diffuser inlet, δ_1, was equal to 0.045 times H_0.

The difference between C_{pi} and C_{pt} is due to primary and secondary effects of friction. In the first place shear stress at the walls causes a loss in pressure. By summing up the calculated shear stress along the wall we have determined the loss in C_{pi} due to friction at the walls. This is shown in Fig. 1 by the broken curve marked C_f which is C_{pi} minus the C_p loss due to wall friction. The difference between the C_f curve and the C_{pt} curve is due to the fact that the area ratio seen by the flow is smaller than the geometric area ratio. This decrease in the effective area ratio seen by the flow is due to the blockage produced by the growth in nonuniformity of the velocity distribution.

As the flow proceeds down the diffuser the boundary layer grows causing larger and larger deviations from the uniform velocity profile assumed in the calculation of C_{pi}. The nonuniformity in the velocity profile caused by friction is amplified by the rising pressure in the decelerating flow. That is the fast moving fluid along the outer edge of the boundary layer has to slow down less than the slower moving fluid near the wall to overcome the same rise in pressure. We shall call this, pressure rise-velocity profile-stretching. To exhibit the significance of this effect as compared to the effect due to friction, we consider the following comparison. The blockage calculated from theory at the diffuser exit, for the various area ratios considered, is shown in Fig. 1. The blockage, B, is defined as

$$B = 1 - \frac{A_{eff}}{A_g} \quad ,$$

where A_g is the geometric diffuser area and A_{eff} the effective area seen by the flow. A_{eff} is calculated by dividing the mass flow rate by the product of the centerline density and velocity. We note, for later use, that for a channel with width much larger than its height, H, the blockage can be approximately written as,

$$B = \frac{\delta_1}{H} \quad ,$$

where δ_1 is the displacement thickness. The exit blockage shown in Fig. 1 is much larger than that caused by the frictional boundary layer growth alone (for fully developed turbulent flow between parallel plates the blockage is 0.125 if we assume the velocity varies as 1/7 power law). Thus the increase in blockage due to pressure rise-velocity profile-stretching is significant. It is also this increase in blockage caused by pressure rise-velocity profile-stretching that is responsible for the ever increasing difference between C_{pi} and C_{pt} as the area ratio increases, even though the loss in C_p due to friction at the walls decreases with increasing area ratio as shown in Fig. 1 by the decreasing difference between C_{pi} and C_{pf}.

The difference between C_{pt} and C_{pm} is due to partial flow separation that occurs in the real flow but is not accounted for in the theoretical calculations. It is this partial separation that at first gradually increases with AR and then eventually grows into a two-dimensional stall that makes it difficult to theoretically predict the diffuser performance. The separation phenomenon in straight wall diffusers is different from that in flow past an airfoil at large angles of attack where the flow separates abrupty across the whole span of the airfoil. In straight wall diffusers (except for very large area ratio diffusers that have little practical interest) there is no abrupt flow

separation across the entire diffuser wall. Instead one talks in terms of the degree of flow separation based upon the fraction of diffuser wall area from which the flow has separated. Guided by the experimental data, Moore and Kline [7], and Fox and Kline [8] in their pioneering works developed the concepts of various diffuser flow regimes based on the degree of flow separation. In our work we have adopted their classification. In particular the flow regime lines for no appreciable stall and large transitory stall wherever indicated in our figures were taken from Fig. 2 of Ref. [5].

From the proceeding discussion we see that if one is to theoretically predict the performance of a diffuser one must in the first place be able to determine from the calculated flow properties when a desired flow regime (no appreciable stall, maximum C_p, etc.) has been reached, i.e., a correlation between some calculated flow parameter and the desired flow regime. And secondly, if possible, estimate the loss in calculated C_{pt} due to the partial separation.

In the following discussion and in the figures, whenever comparing our calculations with the experimental data reported in Refs. [1,2,3] we have indicated blockage by its approximation δ_1/H. This was done to conform to the definition of the blockage used by these authors who carried out their diffuser experiments in large aspect ratio rectangular channels.

CORRELATION OF DIFFUSER FLOW REGIMES WITH CALCULATED FLOW PARAMETERS

The first effort along these lines was made by Reneau [9]. He correlated the line of no appreciable stall with $d\delta_2/dx$, the streamwise gradient of boundary layer momentum thickness. He found that for diffusers with small inlet blockage the line of no appreciable stall is reached when $d\delta_2/dx$ reaches a value of approximately 0.012. This criterion did not work for diffusers with appreciable inlet blockage. Our own computations confirmed Reneau's conclusions. In Fig. 2 we have presented C_{pi}, C_{pt}, etc., for diffuser flow with small inlet blockage; δ_1/H_0 equal to 0.007. Values of experimental C_{pm} were taken from Ref. [1]. Also plotted is our calculation of $d\delta_2/dx$ at the diffuser exit. We find that $d\delta_2/dx$ is indeed equal to about 0.012 at the line of no appreciable stall. However no such correlation was obtained for diffusers with large inlet blockage.

All our efforts to correlate the boundary layer shape factor with flow separation failed. The separation criterion developed by Stratford [10] also did not yield correct results. The reason, we think, is the assumption in Stratford's analysis that close to the separation point the velocity profile very close to the wall varies as

$$u \approx Z^{.5}$$

where Z is the distance from the wall. Our computatons, as will be seen later, show that the partial separation in diffusers starts long before the exponent of Z reaches the value of 0.5.

In our study the point of maximum C_{pm} is selected for correlation. This is the only flow regime that can be unambiguously identified from the experimental data over the entire range of inlet blockages. The no appreciable stall and large trnasitory stall lines given in Ref. [5] are only for diffusers with small inlet blockage. For high inlet blockage even the line for no appreciable stall can be past the point of maximum C_{pm}; see for example (an extreme case) graph for δ_1/H_0 equal to 0.055 in Fig. 8 where the line of no appreciable stall is denoted by a-a'.

The correlations presented in the past have been based on the global properties of the boundary layer. This was necessary since the boundary layer calculations were carried out using variations of the momentum integral approach. In the present work since full viscous calculations are carried out we have explored the local (with respect to distance from the wall) properties of the boundary layer for a correlation parameter.

To gain insight into the development of the boundary layer in diffusers we studied the calculated velocity profiles at various distances along the diffuser. In Fig. 3 is shown a typical set of such velocity profiles plotted in reduced boundary layer coordinates,

$$u^+ = u\rho/\sqrt{\rho\tau_w}\ , \qquad \text{and} \qquad Z^+ = Z\sqrt{\rho\tau_w}/\mu\ ,$$

where τ_w is the shear stress at the wall, ρ the density, μ the viscosity, u the streamwise velocity, and Z the distance from the diffuser wall normal to the flow. In Fig. 3, θ is the diffuser half angle and X the streamwise distance measured from the diffuser entrance. Dots on the curves represent the computational grid points along which u was computed. We note that the velocity profiles plotted on log-log scale are not straight lines but have

curvature. The curvature increases with X. Similar curves for other values of θ show that the curvature grows more rapidly with X for larger values of θ. To bring out more clearly the curvature of the velocity profiles we have plotted in Fig. 4 the gradient

$$d(\ln u^+) / d(\ln Z^+)$$

as a function of Z/H, where H is the half diffuser height at the given X. It can be easily seen that the velocity distribution

$$u \sim Z^n$$

gives

$$d(\ln u^+) / d(\ln Z^+) = n$$

Thus we can look at the curves in Fig. 4 as showing variation of n with Z, if the velocity distribution is locally (in terms of Z) approximated by $u \sim Z^n$.

In our search for a parameter to correlate with maximum C_p we found that the value of n representative of the very near wall region velocity profile gave the best correlation. To be more precise the correlation parameter m presented in this work is the average value of n over the first four grid points (marked 2,3,4, and 5 in Fig. 3). This average was obtained from the slope of the line drawn, using regression analysis, through the points 2,3,4, and 5 on $\ln u^+$ versus $\ln Z^+$ curves. Calculations of m were carried out by putting additional statements in our computer program.

For a given diffuser geometry and inlet conditions, we found that m increases monotonically with X, the distance from the diffuser entrance. The rate of increase of m with X increases with diffuser half angle and the inlet blockage. In Figs. 5 and 6 we have shown variations of the

parameter m with X for different values of diffuser half angle. Figure 5 is for inlet blockage, δ_1/H_0, equal to 0.045 and Fig. 6 is for δ_1/H_0 equal to 0.007.

To determine the correlation between m and C_{pm} maximum we plotted m and C_{pm} versus AR on the same graph. This was done for different sets of values of $L/2H_0$ and δ_1/H_0. Typical curves of such comparison are shown in Figs. 7, 8 and 9. Also shown in these figures is the calculated C_{pt} as a function of AR. Figure 7 shows the comparison for diffusers of different lengths, $L/2H_0$, but all with the same inlet blockage, i.e., with δ_1/H_0 equal to 0.007; the experimental data for C_{pm} is from Ref. [1]. Figure 8 is for diffusers with different inlet blockages, but all of the same length, $L/2H_0$, equal to 12; the experimental data is from Ref. [2]. Figure 9, once again, shows the comparison for diffusers of different lengths but all with the same inlet blockages equal to 0.12 (highest inlet blockage investigated in this study); the experimental data is from Ref. [4].

From our studies of comparison of C_{pm} and m versus AR, we conclude that a value of m equal to 0.22 gives satisfactory correlation with C_{pm} maximum over the entire range of $L/2H_0$, area ratio, and δ_1/H_0 investigated.

Using the criterion that m equal to 0.22 corresponds to maximum C_p we have theoretically generated locus of C_p maximum on AR versus $L/2H_0$ graphs. Results are shown in Figs. 10 and 11. Also shown in these figures are presently calculated and experimentally measured contours of constant C_p. Figure 10 is for the smallest inlet blockage, i.e., δ_1/H_0 equal to 0.007, investigated in the present studies. Figure 11 is for the highest inlet blockage, equal to 0.12, studied. In assessing how well the proposed criterion predicts the area ratio that corresponds to maximum C_p for a given $L/2H_0$, please note that in Figs. 10 and 11 the point on a constant C_{pm} curve that corresponds

to C_{pm} maximum for a given $L/2H_0$ is the point where this curve is tangent to a constant $L/2H_0$ line.

For small inlet blockage, the line of no appreciable stall is well established (see for example Fig. 2 of Ref. [5]). In our studies, we also investigated correlation between the value of m and the line of no appreciable stall, for inlet blockage equal to 0.007. We found that for this inlet blockage value of m equal to 0.18 correlated well with the line of no appreciable stall.

REDUCTION IN EFFECTIVE AREA DUE TO PARTIAL SEPARATION

From our comparisons of C_{pt} and C_{pm} versus AR curves, such as shown in Figs. 7, 8, and 9, we found that in the range in which C_{pm} is less than C_{pm} maximum, C_{pm} is well below C_{pt} at low inlet blockages, and that C_{pm} approaches C_{pt} as the inlet blockage increases. This implies that at low inlet blockage separation initiates well before C_{pm} maximum and moves towards C_{pm} maximum with increasing inlet blockage. Thus, at high inlet blockage one would expect C_{pt} and C_{pm} to be nearly equal. In some of the cases with high inlet blockage C_{pt} was found to be smaller than C_{pm}, for C_{pm} less than C_{pm} maximum. Probably, the reason for C_{pt} being less than C_{pm} is that the inlet boundary layer velocity distributions in the experimental studies were somewhat different than those modeled in our calculations. The flow in a diffuser is dependent on the inlet velocity distribution. Greater the boundary layer thickness at the inlet (i.e., greater the inlet blockage) greater will be the impact on C_p of any differences between the experimental inlet velocity distributions and those modeled in our calculations. In our calculations the velocity distribution within the boundary layer at the diffuser inlet was taken to vary as Z to the power 1/7. The boundary layer thickness was adjusted to meet the inlet blockage requirement. In the experimental setups the blockages was introduced by attaching lead channels of varying lengths upstream of the diffuser inlet to grow the boundary layer to give the desired inlet blockage.

To provide a measure for the reduction in effective area (normal to the flow) caused by the partial flow separation we define,

$$A_t^r = \frac{1}{\sqrt{1 - C_{pt}}}, \qquad \text{and} \qquad A_m^r = \frac{1}{\sqrt{1 - C_{pm}}}$$

We note that A_t^r represents the effective area ratio seen by the computed flow, and A_m^r represents the effective area ratio seen by the actual flow. We now introduce,

$$\Sigma = \frac{A_t^r - A_m^r}{AR}$$

to represent the reduction in the effective flow area caused by the partial flow separation.

In Fig. 12 we have plotted Σ at the point of maximum C_{pm} as a function of inlet blockage, B_i. For inlet blockage greater than about 0.05 calculated C_{pt} is about the same as the actual C_{pm} at maximum C_{pm}. For inlet blockage smaller than 0.05, Fig. 12 can be used, along with the definitions of A_t^r and A_m^r, to determine peak C_{pm} from the calculated peak C_{pt}.

A systematic study of Σ as a function of AR was carried out for the case of inlet blockage, δ_1/H_0, equal to 0.007. This is the case most extensively studied experimentally [1]. The results of the calculation are shown in Fig. 13 in the form of Σ versus AR on log-log scale, for various values of $L/2H_0$. Also shown in this figure is a line passing through area ratios corresponding to C_{pm} maximum. We note that irrespective of the diffuser length, Σ grows smoothly as some power to AR. All the results shown in Fig. 13 are for flows below the flow regime "Fully Developed Two-Dimensional Stall" as given in Fig. 2, Ref. [5]. Results shown in Fig. 13 along with the definitions of A_t^r and A_m^r can be used to determine C_{pm} that corresonds to a calculated C_{pt}.

The remarkable observation shown in the results presented in Fig. 13 is that flow separaton in diffusers, at least below the flow regime of two-dimensional

stall, is a gradual phenomenon even through the point of maximum C_{pm}. There is no abrupt change in the flow separation pattern associated with C_{pm} maximum. Up to the point of C_{pm} maximum the reduction in the effective area as seen by the flow due to the flow separation is less than the increase due to the increase in the area ratio and therefore C_{pm} increases. Beyond C_{pm} maximum a given increase in the area ratio introduces a larger increase in the flow separated area resulting in net decrease in the effective area seen by the flow and an associated decrease in C_{pm}.

CONCLUDING REMARKS

Based on the results presented in the last two sections, one can construct various algorithms, depending upon the design specifications, to calculate the optimum diffuser geometries. For example, if the inlet conditions (inlet diffuser dimensions and the inlet flow conditions) and the diffuser length, L, are specified one can calculate the diffuser half angle (or the area ratio) for maximum pressure recovery as follows. Pick a value for the half angle, θ, and starting with the given inlet conditions calculate C_{pt} and m at the diffuser exit (i.e., at X equal to L). Repeat the calculations with larger and larger values of θ until the value of m at the diffuser exit becomes equal to or greater than 0.22. Plot θ and C_{pt} versus m. The value of θ that corresponds to m equal to 0.22 is the desired half angle for the maximum pressure recovery. The value of C_{pt} that corresponds to m equal to 0.22 is the maximum theoretical pressure recovery. From this C_{pt} maximum, and the given inlet conditions we can now estimate C_{pm} maximum using the results given in Fig. 12.

APPENDIX A -- NOMENCLATURE

L = diffuser length

H = half the distance between the diverging diffuser walls

W = half the distance between the parallel walls

H_0 = H at the inlet

X = distance along the diffuser centerline

Z = distance from the diffuser wall normal to the flow

A_g = geometric diffuser area

A_{eff} = diffuser area obtained by dividing the mass flow rate by the product of the centerline density and velocity

p_e = diffuser exit pressure

p_i = diffuser inlet pressure

p_{0i} = diffuser inlet stagnation pressure

C_p = pressure recovery coefficient

C_{pi} = ideal C_p

C_{pt} = calculated C_p

C_{pm} = measured C_p

AR = diffuser geometric area ratio

$A_t^r = 1/\sqrt{1 - C_{pt}}$, effective area ratio seen by the calculated flow

$A_m^r = 1/\sqrt{1 - C_{pm}}$, effective area ratio seen by the actual flow

B = blockage $= 1 - \frac{A_{eff}}{A_g} \approx \frac{\delta_1}{H}$ for large aspect ratio diffusers

u = streamwise velocity

u^+, z^+ = reduced boundary layer coordinates

n = exponent of Z in $u \sim Z^n$

m = average value of n in the very near wall region

θ = diffuser half angle

δ_0 = boundary layer thickness

δ_1 = boundary layer displacement thickness

δ_2 = boundary layer momentum thickness

τ_w = local wall shear stress

ρ = density

μ = viscosity

APPENDIX B -- COMPUTATIONAL METHODOLOGY

Diffuser calculations were carried out using the method of Ref [6]. In this method the flow in the channel is divided into finite streams and the finite difference equations are then obtained by applying conservation principles directly to the individual streams. The resulting finite difference equations, solution technique, and the turbulence model used (based on the mixing length hypotehsis) are all given in Ref. [6]. Here we discuss two points of special significance to the present study.

GRID SPACING

Let Z_1 be the wall. The next grid point Z_2 is selected such that the local Reynold's number along Z_2. i.e.

$$\frac{u_2 Z_2}{\text{kinematic viscosity}}$$

is equal to 1200. This places Z_2 just outside the laminar sublayer and the transition zone. The grid point Z_j is calculated from the relation

$$Z_j = Z_2 + (H_0 - Z_2)(j/N)^G$$

where N is the total number of grid points (21 in the present calculations), and the exponent G is calculated from the requirement,

$$Z_3 - Z_2 = Z_2 - Z_1$$

EFFECT OF PARALLEL WALLS

Let W be half the distance between the parallel walls. The effect of parallel walls was taken into account by using W_c instead of W in the calculations. W_c is defined as

$$W_c = W - \delta_1 \qquad \text{for } \delta_0 \leq W, \quad \text{and}$$

$$W_c = W\left(1 - \frac{\delta_1}{\delta_0}\right) \qquad \text{for } \delta_0 > W$$

where δ_0 and δ_1 are the boundary layer thickness and the displacement thickness computed along the diverging walls.

For large aspect ratio ($W \gg H_0$), as for the Refs. 1, 2, and 3 cases, the proceeding correction to W is not very crucial, although it was incorporated in our computations. However for an aspect ratio of one at the inlet, as for the Ref. 4 case, the proceeding correction is essential.

ACKNOWLEDGEMENTS

We would like to thank Dr. John M. Smith of NASA-Lewis Research Center for his valuable discussions and suggestions during the course of this work. The work was supported by NASA/DOE Grant NSG-3186.

REFERENCES

1. E.G. Reid, "Performance Characteristics of Plane-Wall Two-Dimensional Diffusers," NACA TN 2888, February, 1953.

2. B.A. Waitman, L.R. Reneau, and S.J. Kline, "Effects of Inlet Conditions on Performance of Two-Dimensional Diffusers," Report PD-5, Department of Mechanical Engineering, Stanford University, March, 1960.

3. L.R. Reneau, "Performance and Design of Straight Two-Dimensional Diffusers," Engineer's Thesis, Department of Mechanical Engineering, Stanford University, January, 1965.

4. P.W. Runstadler, Jr., and R.C. Dean, Jr., "Straight Channel Diffuser Performance at High Inlet Mach Numbers," Journal of Basic Engineering, Trans. ASME, Series D, Vol. 91, No. 3, September 1969, pp. 397-422.

5. L.R. Reneau, J.P. Johnston, and S.J. Kline, "Performance and Design of Straight Two-Dimensional Diffusers," Journal of Basic Engineering, Trans. ASME, Series D, Vol. 89, No. 1, March 1967, pp. 141-150.

6. M.S. Greywall, "Streamwise Computation of Duct Flows," Computer Methods in Applied Mechanics and Engineering, Vol 21, February 1980, pp. 231-247.

7. C.A. Moore and S.J. Kline, "Some Effects of Vanes and of Turbulence on Two-Dimensional Wide-Angle Subsonic Diffusers," NACA TN 4080, June 1958.

8. R.W. Fox and S.J. Kline, "Flow Regime Data and Design Methods for Curved Subsonic Diffusers," Journal of Basic Engineering, Trans. ASME, Series D, Vol. 84, 1962, pp. 303-312.

9. L.R. Reneau and J.P. Johnston, "A Performance Prediction Method of Unstalled Two-Dimensional Diffusers," Journal of Basic Engineering, Trans. ASME, Vol. 89, 1967, pp. 643-654.

10. B.S. Stratford, "The Prediction of Separation of the Turbulent Boundary Layer," Journal of Fluid Mechanics, Vol. 5, 1959, pp. 1-16.

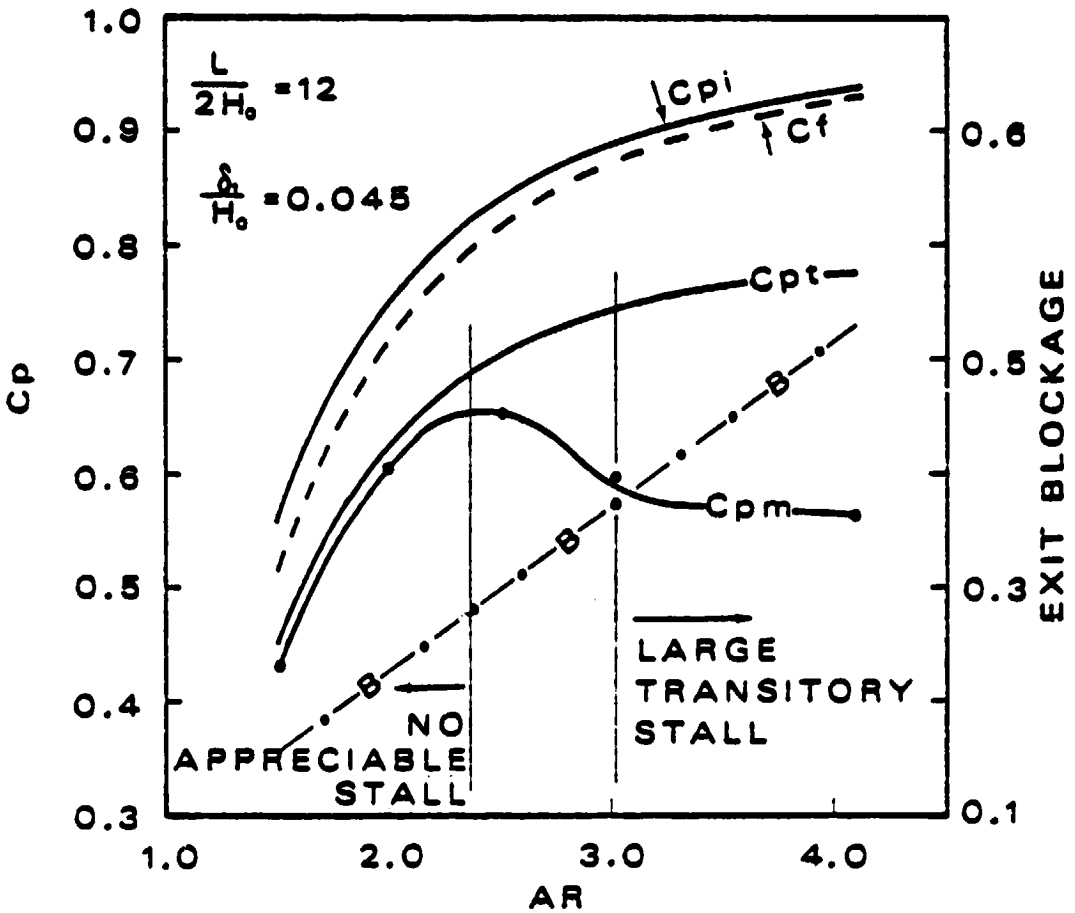

Figure 1 - Ideal, C_{pi}, calculated, C_{pt}, and measured, C_{pm}, pressure recovery coefficients as functions of diffuser area ratio. Curve marked C_f is C_{pi} minus C_p loss due to friction at the walls. Also shown is the blockage, B, at the diffuser exit as a function of AR.

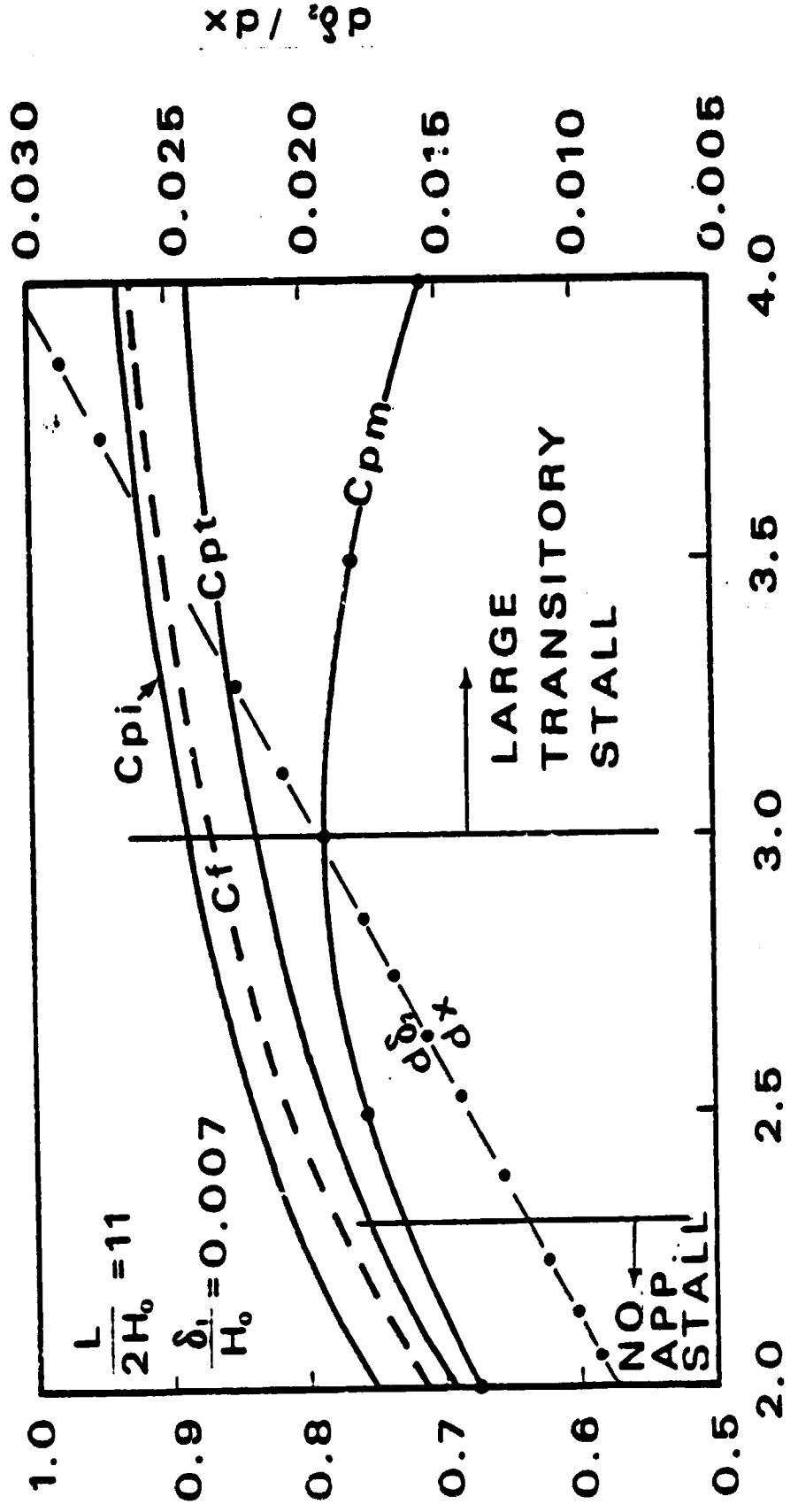

Figure 2 - Ideal, C_{pi}, calculated, C_{pt}, and measured, C_{pm}, pressure recovery coefficients as functions of diffuser area ratio. Curve marked C_f is C_{pi} minus C_p loss due to friction at the walls. Also shown is the axial gradient of the boundary layer momentum thickness, $d\delta_2/dx$, at the diffuser exit as function of AR.

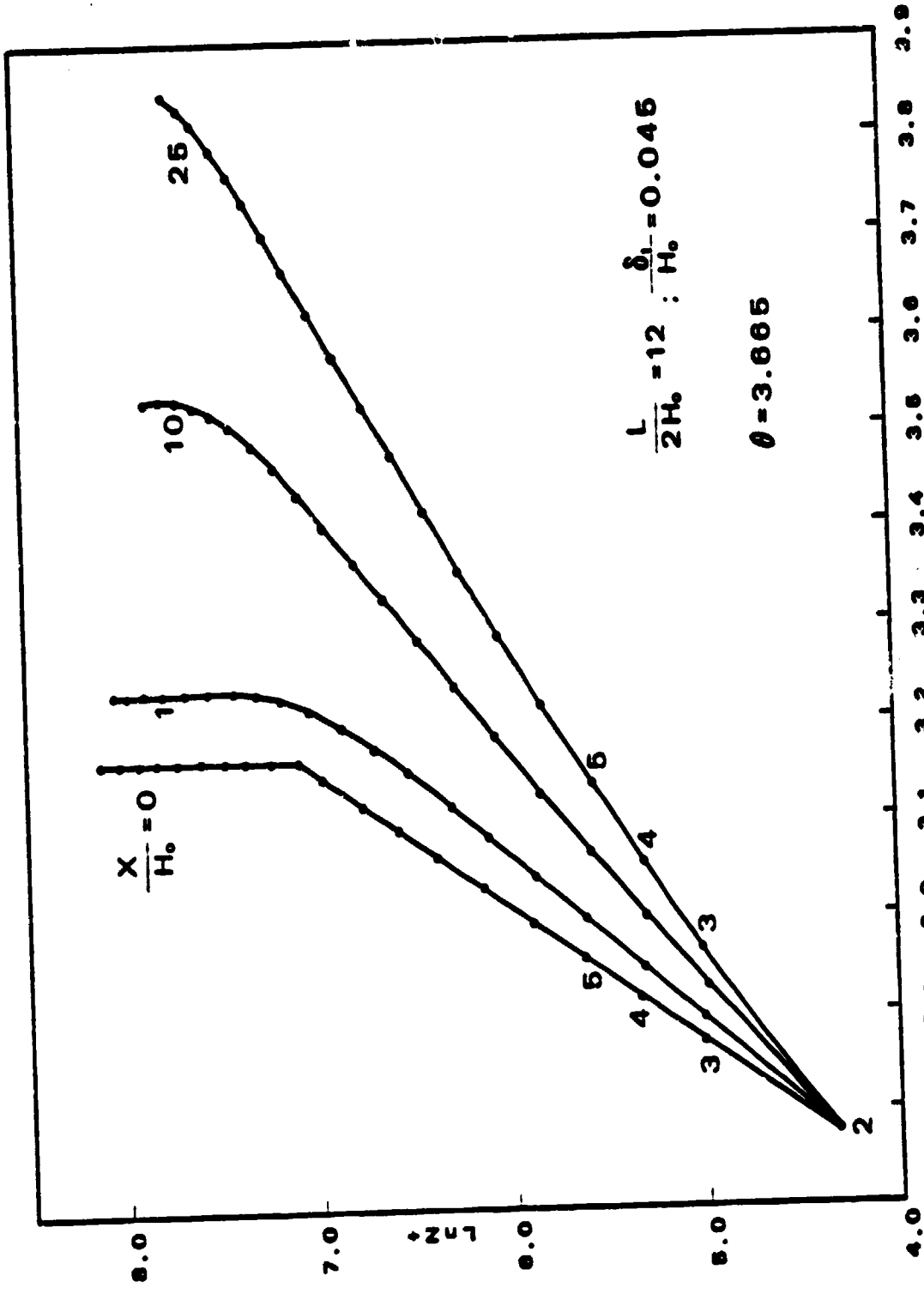

Figure 3 - Boundary layer velocity distribution at axial distance X/H_0 equal to 0, 1, 10, and 25.

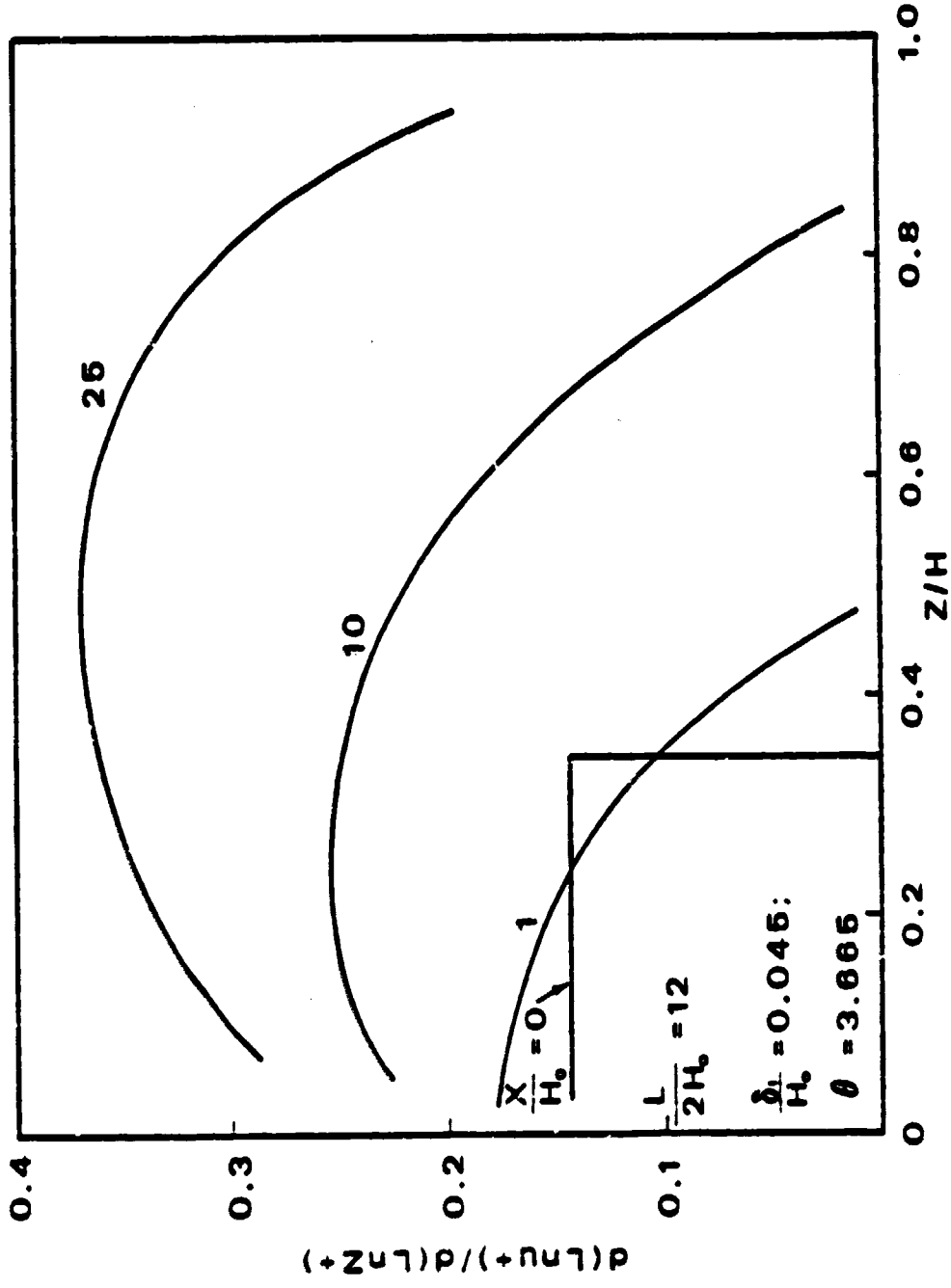

Figure 4 - Distribution of the boundary layer velocity profile gradient along the distance Z from the wall at four locations along the diffuser.

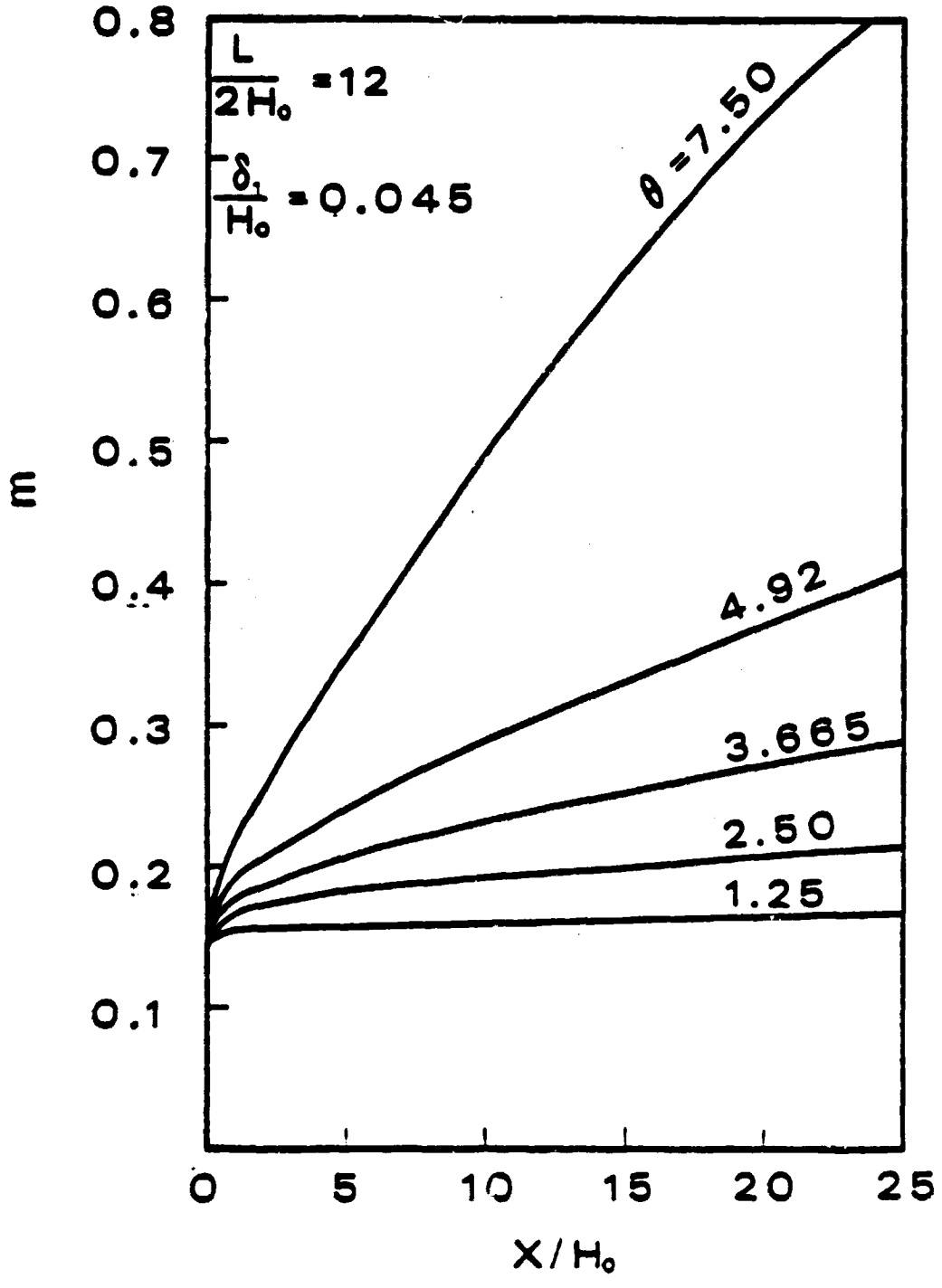

Figure 5 - Growth of m along the diffuser for various values of diffuser half angle for inlet blockage equal to 0.04[illegible]

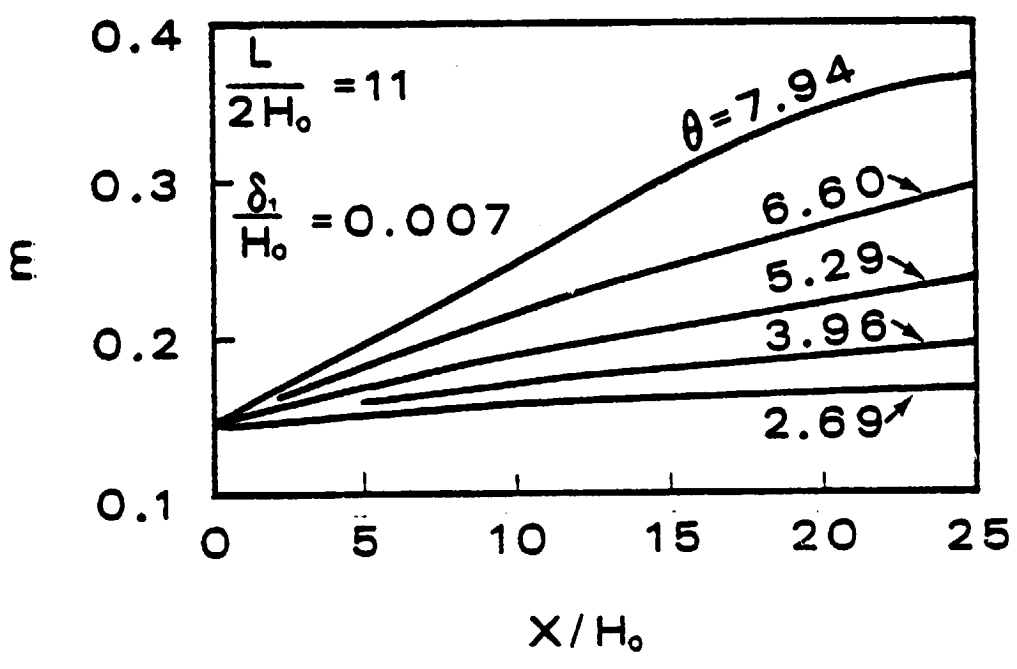

Figure 6 - Growth of m along the diffuser for various values of diffuser half angle for inlet blockage equal to 0.007.

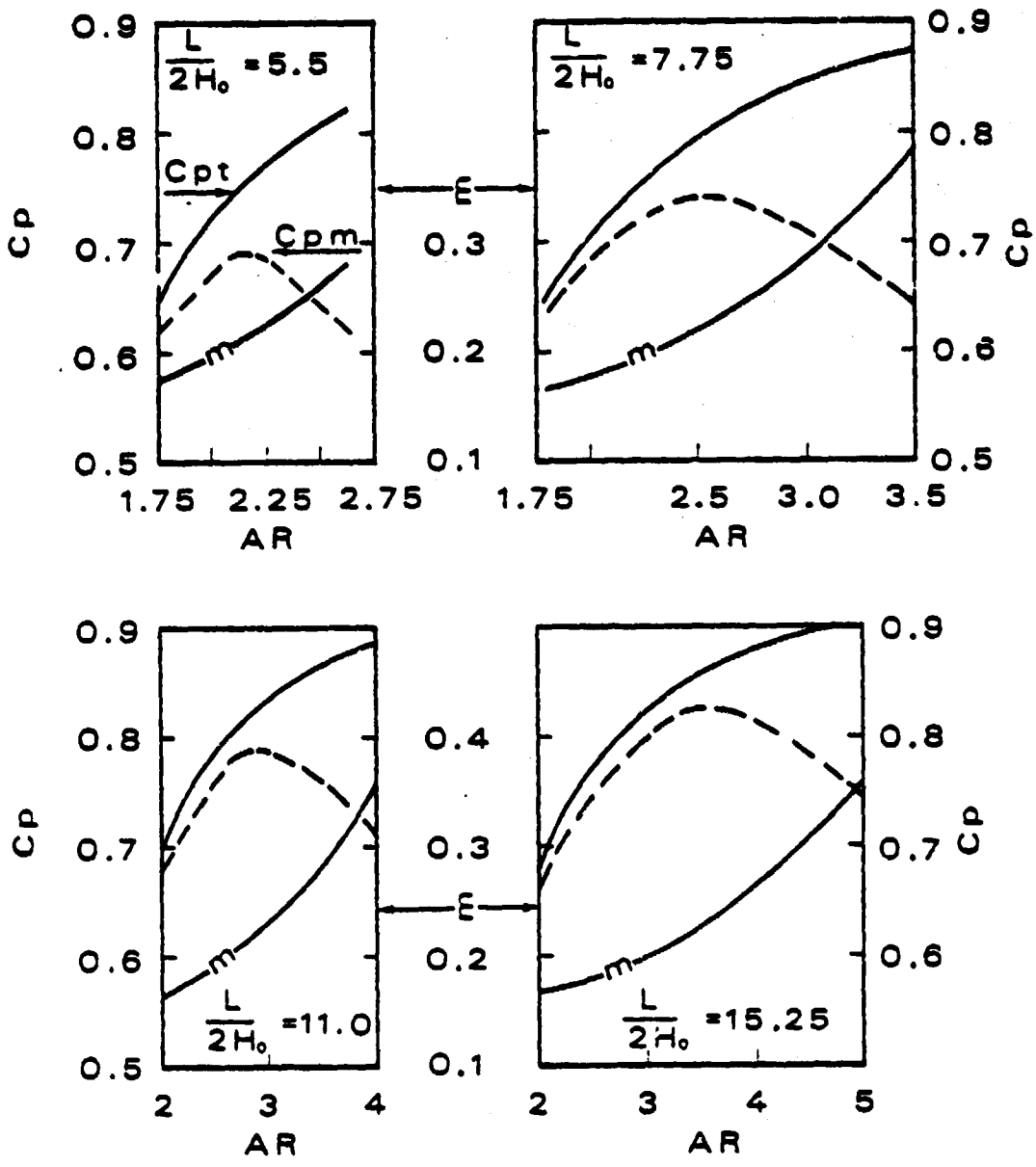

Figure 7 - Distributions of C_{pt}, C_{pm} from Reference 1. and m as functions of AR for different diffuser lengths, $L/2H_0$. Inlet conditions: blockage = 0.007; aspect ratio = 8; velocity = 69 m/s; fluid-air at N.T.P.

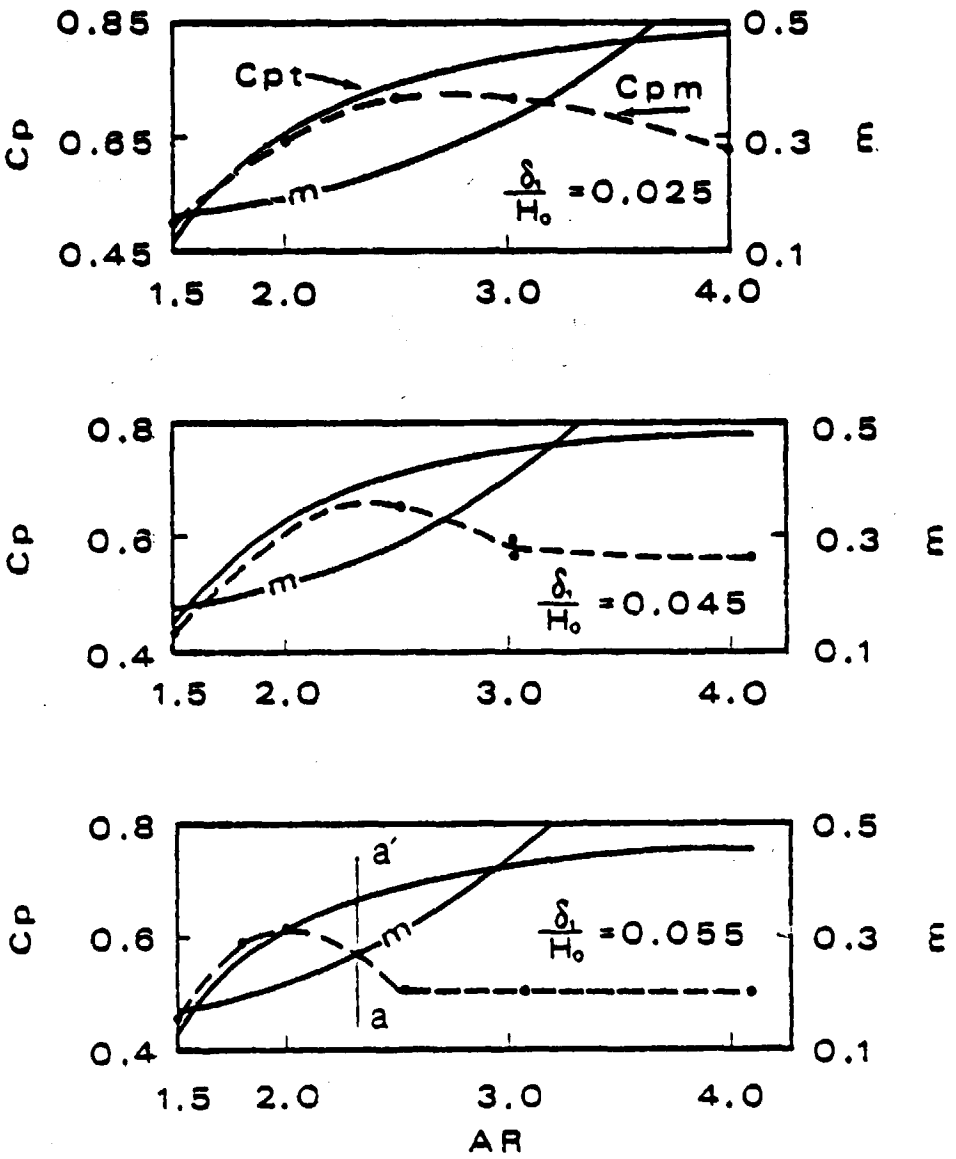

Figure 8 - Distributions of C_{pt}, C_{pm} from Reference 2, and m as functions of AR for different inlet blockages, δ_1/H_0, for diffuser of $L/2H_0$ equal to 12. Inlet conditions: aspect ratio = 12; velocity = 49 m/s; fluid-air at N.T.P.

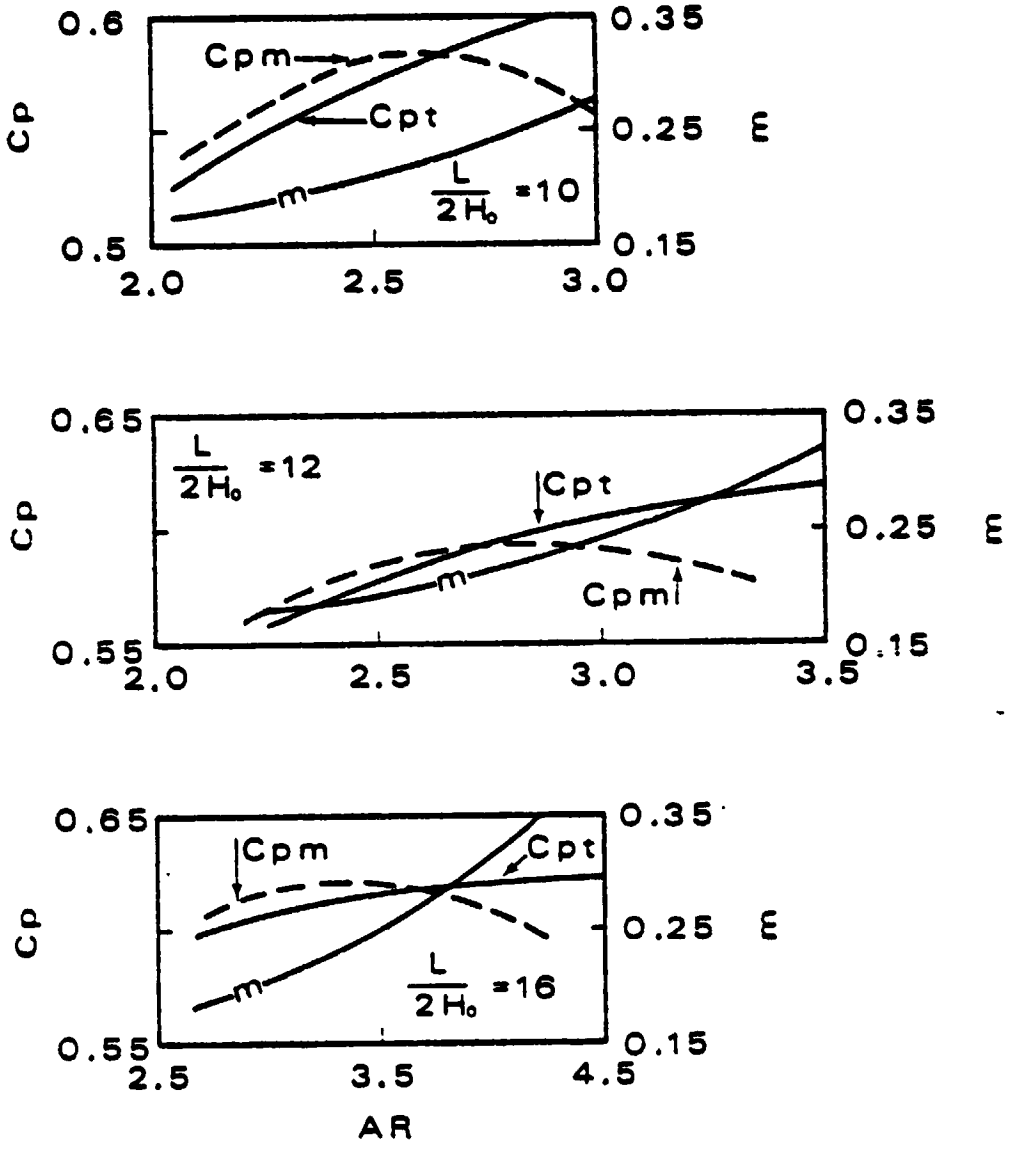

Figure 9 - Distributions of C_{pt}, C_{pm} from Reference 4, and m as functions of AR for different diffuser lengths, $L/2H_0$. Inlet conditions: blockage = 0.12, aspect ratio = 1; Mach = 0.6, fluid-air.

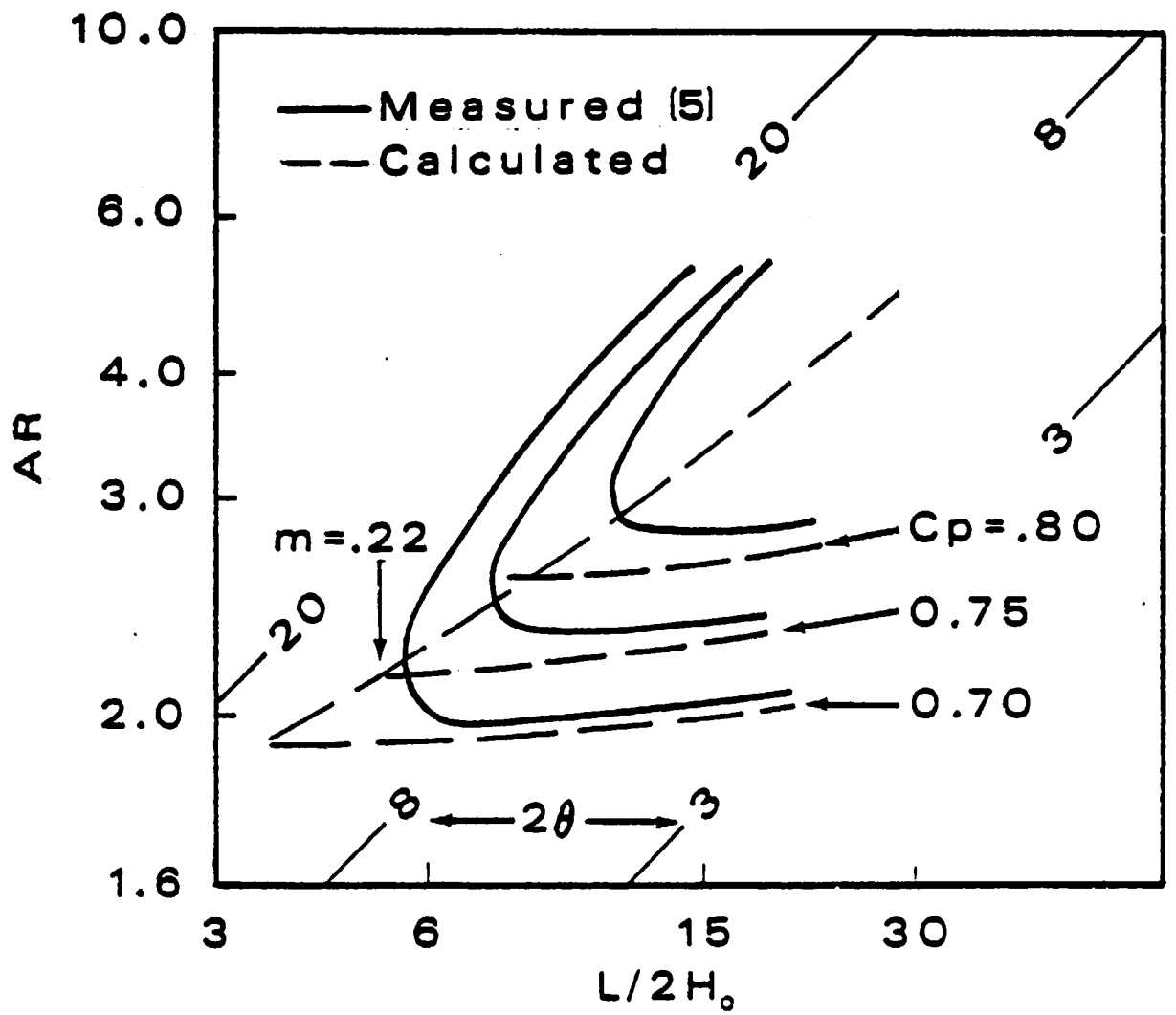

Figure 10 - Measured and calculated contours of constant C_p for inlet blockage equal to 0.007. Also shown is the calculated locus of C_p maximum using the criteria m = 0.22 for C_p maximum.

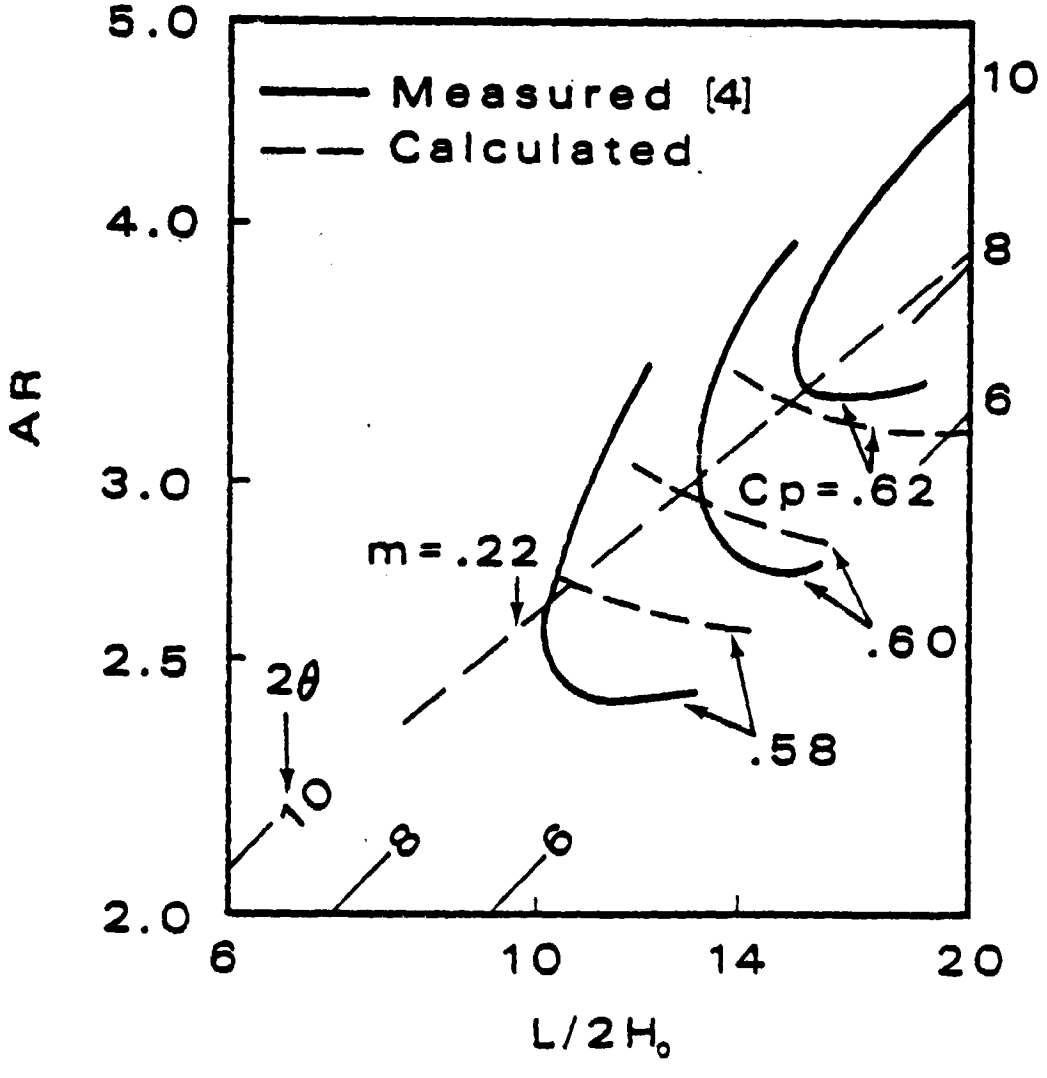

Figure 11 - Measured and calculated contours of constant C_p for inlet blockage equal to 0.12. Also shown is the calculated locus of C_p maximum using the criterion m = 0.22.

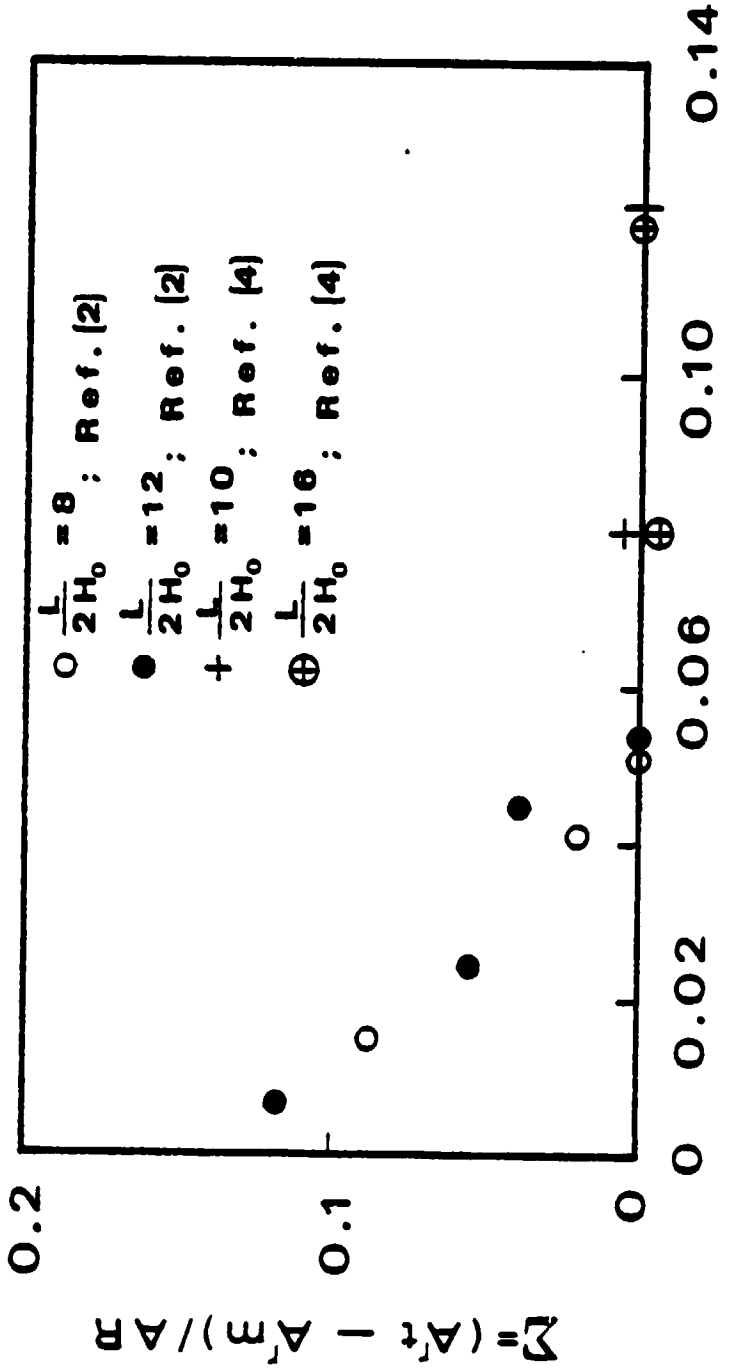

Figure 12 - Reduction, due to partial flow separation, in the effective area seen by the flow, Σ, at the point of maximum C_{pm} as function of inlet blockage, B_i.

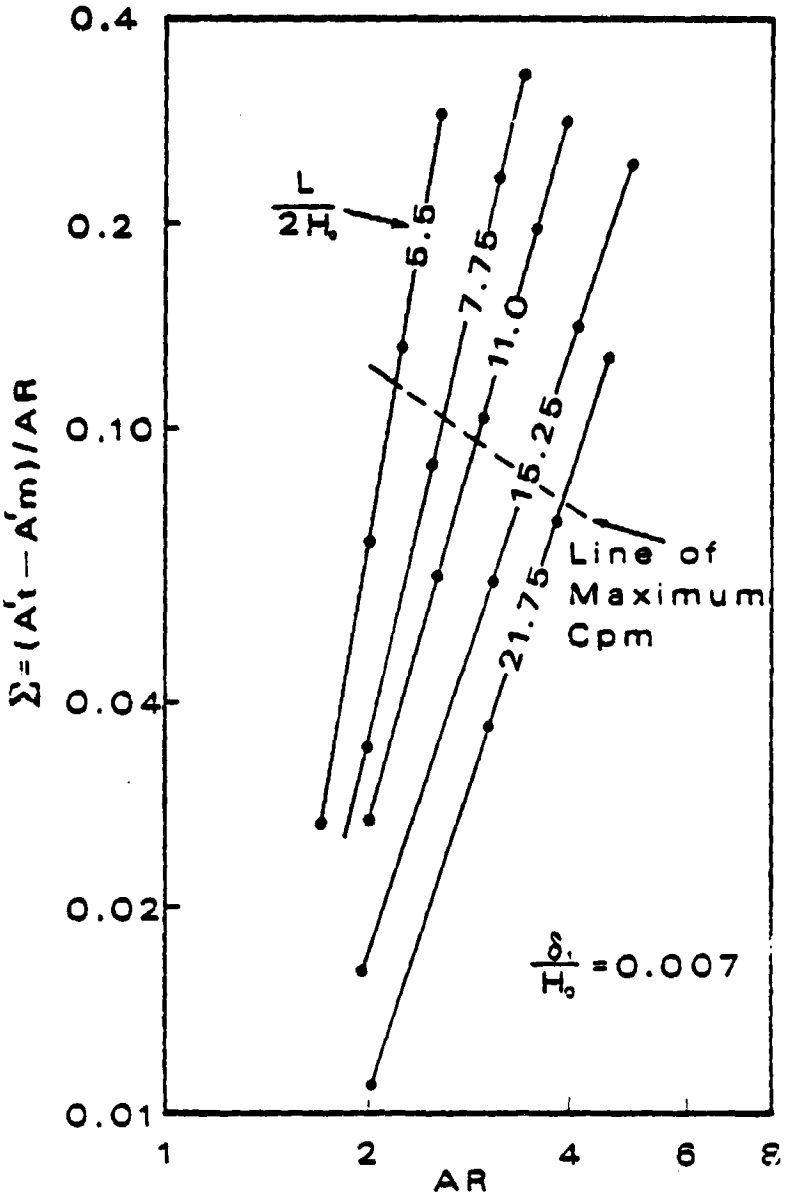

Figure 13 - Reduction, due to partial flow separation, in the effective area seen by the flow, Σ, as function of the diffuser area ratio, AR, for various diffuser lengths.